Ca^{2+}-Triggered Simultaneous Membrane Penetration of the Tandem C2-Domains of Synaptotagmin I

Enfu Hui, Jihong Bai, and Edwin R. Chapman
Howard Hughes Medical Institute and Department of Physiology, University of Wisconsin School of Medicine, Madison, Wisconsin 53706

ABSTRACT Synaptotagmin I (syt), a transmembrane protein localized to secretory vesicles, functions as a Ca^{2+} sensor that facilitates SNARE-mediated membrane fusion. The cytoplasmic domain of syt harbors two C2-domains designated C2A and C2B. Upon binding Ca^{2+}, C2A and C2B partially penetrate into membranes that contain anionic phospholipids. However, it is unknown whether these tandem C2-domains engage membranes at the same time, in a sequential manner, or in a mutually exclusive manner. We have used site-directed fluorescent probes to monitor the penetration of syt's C2-domains into phosphatidylserine-harboring lipid bilayers. We report that, in response to Ca^{2+}, C2A and C2B copenetrate into these bilayers with diffusion-limited kinetics. Membrane penetration was more efficient when synthetic rather than natural phospholipids were used to prepare bilayers. The membrane penetration activity of the intact cytoplasmic domain of syt (C2A-C2B) exhibits significant resistance to changes in ionic strength. In contrast, the ability of isolated C2B to bind membranes in response to Ca^{2+} can be disrupted by subtle changes in ionic strength. Tethering C2B to a mutant version of C2A that does not bind Ca^{2+} or membranes significantly increases the stability of Ca^{2+}·C2B·membrane complexes, confirming that C2A affects the membrane-binding properties of the adjacent C2B domain.

INTRODUCTION

Exocytosis of neurotransmitter is an extremely rapid process that is triggered by influx of Ca^{2+} through voltage-activated Ca^{2+} channels (1–3). The molecular identity of Ca^{2+} sensors that regulate secretion and the molecular mechanism by which these sensors couple Ca^{2+} to the opening of fusion pores are issues that have attracted considerable attention (4). A substantial body of evidence suggests that synaptotagmins, a family of transmembrane proteins localized to secretory vesicles, play critical roles in coupling Ca^{2+} to exocytosis. In particular, synaptotagmin I (syt), the best-characterized member in the family, likely serves as the Ca^{2+} sensor for rapid neurotransmitter release at synapses (4–6).

Syt harbors a short N-terminal luminal domain, a single transmembrane domain, and a large cytoplasmic domain composed of tandem C2-domains, designated C2A and C2B (7,8). It is well established that in response to Ca^{2+}, C2A binds tightly and rapidly to membranes harboring anionic phospholipids, such as phosphatidylserine (PS) (9,10). Two Ca^{2+}-binding loops of C2A (loop 1 and 3) partially penetrate into lipid bilayers, forming a tripartite complex—Ca^{2+} · C2A·membrane—in which anionic phospholipid headgroups probably complete the Ca^{2+}-binding sites to increase the apparent affinity of C2A for Ca^{2+} (10–13). C2B is structurally similar to C2A (14) and also functions as a Ca^{2+}-sensing module (15); however, the biochemical properties of C2A and C2B are distinct from each other (16). Many synaptic components, such as AP-2, Ca^{2+} channels, other copies of syt, and PIP_2 (phosphatidylinositol 4, 5-bisphosphate), interact with C2B but not with C2A (17–22).

Tethering of C2A and C2B equips syt with additional, novel, biochemical properties; namely, both C2-domains are required for syt to efficiently bind SNARE (soluble *N*-ethylmaleimide-sensitive fusion protein attachment protein receptor) proteins, which are components of a conserved membrane fusion machine (10,23–25). Cell-based and reconstitution experiments indicate that syt·SNARE interactions are essential for coupling Ca^{2+} to SNARE-mediated membrane fusion (24,26–31). For example, it has been shown that altering the length of the linker that connects C2A and C2B reduces the interaction of syt with SNAREs and destabilizes exocytotic fusion pores in PC12 cells (30). These data demonstrate that the close physical coupling of the tandem C2-domains is critical for its function during secretion.

Cooperation between tethered C2A and C2B has also been reported for the Ca^{2+}-triggered interaction of syt with liposomes composed of PS and PC (phosphatidylcholine) (32). The functional relevance of the interaction of Ca^{2+}-syt with PS was addressed using a reconstituted, SNARE-mediated membrane fusion assay (24). Omission of PS from SNARE-bearing proteoliposomes completely abrogated the ability of Ca^{2+}·syt to regulate fusion in this assay system (31). Thus, PS is an essential effector for the action of Ca^{2+}·syt. In the context of the intact cytoplasmic domain of syt, C2A-C2B, two Ca^{2+}-binding loops of C2B rapidly penetrate PS-bearing lipid bilayers to form a high affinity complex (20,32). In contrast, studies focused on the isolated C2B domain have resulted in a less conclusive view. For example, only low levels of PS/PC binding were observed in some studies

Submitted December 22, 2005, and accepted for publication June 1, 2006.

Address reprint requests to Edwin R. Chapman, HHMI and Dept. of Physiology, SMI 129, University of Wisconsin, 1300 University Ave., Madison, WI 53706. Tel.: 608-263-1762; Fax: 608-265-5512; E-mail: chapman@physiology.wisc.edu.

Jihong Bai's present address is Massachusetts General Hospital, Dept. of Molecular Biology, Richard B. Simches Research Building, 185 Cambridge St., CPZN-7250, Boston, MA 02114-2790.

0006-3495/06/09/1767/11 $2.00

doi: 10.1529/biophysj.105.080325

(14,28,32,33), whereas robust binding to membranes composed of PS/PC was reported in another study (34). These differences may be due to different experimental conditions and assays used to monitor binding (as detailed in Results).

The interface between the C2-domains of syt and membranes contains positively charged residues that interact with the anionic headgroups of PS (12,13,20). These residues have been mutated and the effects of these mutations characterized at biochemical and functional levels (35,36). Mutation of one of the positively charged residues in either C2A (R233Q) or C2B (K366Q) shifted the Ca^{2+} dependence of C2A-C2B·PS/PC membrane interactions; however, the R233Q/K366Q double mutant did not exhibit a further shift in the Ca^{2+} dependence for binding to PS-bearing liposomes (36); that is, a mutation in C2A seems to reduce the Ca^{2+}-dependent binding of C2B-domain to membranes, and this deficit could not be further exacerbated by an additional analogous mutation in C2B. These data suggest that the R233Q/K366Q mutations disrupt the ability of C2A and C2B to functionally interact or ''cooperate'' with one another. However, these results can also be explained by the possibility that C2A and C2B interact with membranes in a mutually exclusive manner, i.e., C2A and C2B do not penetrate PS/PC membranes at the same time. In this model, once one C2-domain penetrates into PS/PC bilayers, the other C2-domain is rendered unable to dip into lipid bilayers.

Here, using site-directed fluorescent probes, we report that C2A and C2B penetrate into lipid bilayers at the same time. Stopped-flow rapid mixing experiments show that both C2A and C2B, in the context of C2A-C2B, interact with PS/PC membranes with rapid and identical—within the time resolution of the assay—kinetics. In addition, we address the question of whether the isolated C2B domain of syt functions as an efficient PS-binding module (34) or whether this domain must be activated by an adjacent C2A domain (32). The data presented here suggest that the tandem C2-domains of syt synergize in a complex manner to mediate high affinity binding of Ca^{2+}·syt to PS-harboring membranes.

MATERIALS AND METHODS

Recombinant proteins

cDNA encoding rat syt I (G374 version) (15,37) was kindly provided by G. Schiavo (Imperial Cancer Research Fund). The cytoplasmic (designated C2A-C2B, residues 96–421), C2A (residues 96–265), and C2B (residues 248–421) domains of syt I (G374 version) were expressed in *Escherichia coli* as glutathione *S*-transferase fusion proteins and purified by using glutathione-Sepharose beads (Amersham Pharmacia, Piscataway, NJ) as described (23,38). Recombinant syts harbor tightly bound contaminants that may affect their properties (14,33). These bacterial contaminants were removed using DNAase/RNAase and high salt washes as described previously (20). Soluble proteins were generated by thrombin cleavage of their respective GST fusion proteins, as described (38).

In C2A-C2B, the native Cys-277 was replaced with Ala, and a single Cys was introduced in loop 3 of C2A (F234C; designated C2A(3)-C2B), C2B (I367C; designated C2A-C2B(3)), or both C2-domains (designated C2A(3)-C2B(3)). A single Cys was also placed in loop 1 of the C2B domain of C2A-C2B (V304C; designated C2A-C2B(1)) and in loop 1 or loop 3 of the isolated C2B domain (indicated as C2B(1) and C2B(3), respectively). In $C2A_M$-C2B(3) and $C2A_M$-C2B, the subscript M corresponds to D-230, 232N substitutions that disrupt the Ca^{2+} and lipid-binding activity of C2A (39). In C2A-$C2B_M$ and C2A(3)-$C2B_M$, the subscript M corresponds to D-363, 365N substitutions that disrupt the Ca^{2+} and lipid-binding activity of C2B (14). All point mutations were generated using the overlapping primer method as described (40).

In C2B(KK), C2A-C2B(KK), and $C2A_M$-C2B(KK), KK corresponds to K-326, 327A substitutions that neutralize the two lysine residues previously shown to be crucial for the oligomerization activity of C2B (19,33).

cDNA encoding these constructs were subcloned into pGEX-2T (Amersham Pharmacia) using *Bam*HI and *Eco*RI sites, expressed in *E. coli*, and purified as described above.

Fluorescent labeling of C2A-C2B

Cys residues in C2A-C2B were labeled by incubating purified protein with a 10-fold molar excess of 1,5-IAEDANS (5-[[2-[(iodoacetyl) amino] ethyl] amino] naphthalene-1-sulfonic acid) (Molecular Probes, Eugene, OR) at 25°C for 1 h in HEPES buffer (50 mM HEPES, pH 7.4, 0.1 M NaCl; the same buffer was used for all experiments unless otherwise indicated). Free fluorophore was removed by extensive dialysis. The AEDANS concentration was determined using an extinction coefficient of $6.0 \times 10^3\ M^{-1}\ cm^{-1}$ at 337 nm (32,41). The protein concentration was determined by sodium dodecyl sulfate-polyacrylamide gel electrophoresis (SDS-PAGE) and staining with Coomassie brilliant blue using bovine serum albumin as a standard. Labeling ratios were 0.85–0.95 mol label/mole of protein. AEDANS probes on proteins are represented as asterisks (*) in all figures.

Phospholipids

Synthetic 1,2-dioleoyl-*sn*-glycero-3-[phospho-L-serine] (PS), synthetic 1,2-dioleoyl-*sn*-glycero-3-phosphocholine (PC), 1-palmitoyl-2-stearoyl (5-doxyl)-*sn*-glycero-3-phosphocholine (5-doxyl-PC), 1-palmitoyl-2-stearoyl (7-doxyl)-*sn*-glycero-3-phosphocholine (7-doxyl-PC), and 1-palmitoyl-2-stearoyl (12-doxyl)-*sn*-glycero-3-phosphocholine (12-doxyl-PC), brain-derived PS, brain-derived PC, and 1,2-dioleoyl-*sn*-glycero-3-phosphoethanolamine-*N*-(5-dimethylamino-1-naphthalenesulfonyl) (dansyl-PE) were obtained from Avanti Polar Lipids (Alabaster, AL).

Liposomes

Phospholipids were dried under a stream of nitrogen and suspended in HEPES buffer. For fluorescence studies, large (~100 nm) unilamellar liposomes were prepared by extrusion as described previously (10).

Fluorescence measurements

Steady-state fluorescence measurements were performed at 25°C using a PTI (South Brunswick, NJ) QM-1 fluorometer with FELIX software. Labeled protein (0.5 μM) was mixed with liposomes (11 nM liposomes or 1 mM total phospholipids) in a cuvette using a castle-style stir bar. AEDANS was excited at 336 nm, and emission spectra were collected from 420 to 600 nm (2-nm slits) and were corrected for blank, dilution, and instrument response. $[Ca^{2+}]_{free}$ was calculated using WEBMAXC 2.22 software (C. Patton, Stanford University, Stanford, CA). For the quenching experiments shown in Supplementary Fig. 1, liposome composition was 25% PS, 65% PC, and 10% doxyl-PC; the doxyl group was placed at the 5-, 7-, or 12-position of the *sn*-2 acyl chain.

The depth of penetration of the AEDANS probe was addressed using the parallax method (13,42). The distance of the fluorescent probe (i.e., AEDANS) from the center of the lipid bilayer (Z_{CF}) is described by Eq. 1:

$$Z_{CF} = L_{C1} + [-\ln(F_1/F_2)/\pi C - L^2]/2L,$$

where L_{C1} represents the distance from the bilayer center to the shallow quencher (12.2 Å for 5-doxyl-PC) (43), C is the mole fraction of the quencher divided by the lipid area (70 Å^2), F_1 and F_2 are the relative fluorescence intensities of the shallow (5-doxyl-PC) and deep quenchers (12-doxyl-PC), respectively, and L is the difference in the depth of the two quenchers (0.9 Å per CH_2 group). For this analysis we assumed that the thicknesses of the hydrophobic and hydrophilic regions of one leaflet of the bilayer are 10 Å and 15 Å, respectively (44).

Stopped-flow rapid mixing experiments

Rapid mixing experiments were carried out using an Applied Photophysics (Leatherhead, UK) SX.18MV stopped-flow spectrometer at 25°C (10). AEDANS-labeled proteins, in HEPES buffer, were excited at 336 nm, and emitted light was collected using a 470-nm cutoff filter. For fluorescence resonance energy transfer (FRET) experiments, native tryptophan residues in C2A-C2B (2 μM) were excited at 285 nm and the emission from dansyl-PE was collected using a 523-nm band-pass filter. The dead time of the instrument was ~1.2 ms. The on-rates (k_{on}) and off-rates (k_{off}) for the interaction of Ca^{2+}·C2A-C2B with liposomes were calculated, assuming pseudo-first-order kinetics (10), according to Eq. 2:

$$k_{obs} = [\text{liposome}]k_{on} + k_{off}.$$

Cosedimentation assays

Large (~100 nm) unilamellar liposomes were prepared using synthetic phospholipids (25% PS/75% PC). Syt fragments (3 μM) were incubated with liposomes (22 nM liposomes or 2 mM total phospholipids) in 100 μl of HEPES buffer for 15 min at room temperature, in the presence of 1 mM Ca^{2+} or 2 mM EGTA. Samples were then centrifuged at 150,000 × g at 4°C for 40 min in a Beckman Optima MAX-E (Beckman Coulter, Fullerton, CA) tabletop ultracentrifuge, and the supernatants and pellets were collected. Pellets were washed once with 100 μl of HEPES buffer and collected again via centrifugation. Equal fractions of the supernatant and pellet from each sample were subjected to SDS-PAGE, and proteins were visualized by staining with Coomassie brilliant blue.

RESULTS

Site-directed probes have been used to gain insight into the mechanism and kinetics by which Ca^{2+}·syt engages membranes. These studies revealed that in response to Ca^{2+}, the Ca^{2+}-binding loops of both C2A and C2B, in the context of the intact cytoplasmic domain (designated C2A-C2B), penetrate membranes that contain anionic phospholipids (10,13, 20,32). However, it was not clear whether Ca^{2+}·C2A-membrane and Ca^{2+}·C2B-membrane interactions occur simultaneously, with distinct kinetics, or in a mutually exclusive manner.

To address these issues, we used a site-directed fluorescent probe, AEDANS, to label Ca^{2+}-binding loop 3 of C2A or C2B (indicated as C2A*(3)-C2B or C2A-C2B*(3), respectively, as shown in Fig. 1 *A*, *upper panel*). Results from steady-state fluorescence measurements using these constructs are consistent with previous studies (20,32). Both C2A*(3)-C2B and C2A-C2B*(3) exhibited a Ca^{2+}-dependent increase in fluorescence intensity and a blue-shift in the emission spectrum when mixed with liposomes that harbored the anionic phospholipid PS (25% PS/75% PC) (Fig. 1, *A* and *B*, *lower panel*). These changes in the emission spectrum report the Ca^{2+}-triggered penetration of the Ca^{2+}-binding loops of C2A and C2B into the lipid bilayer (20).

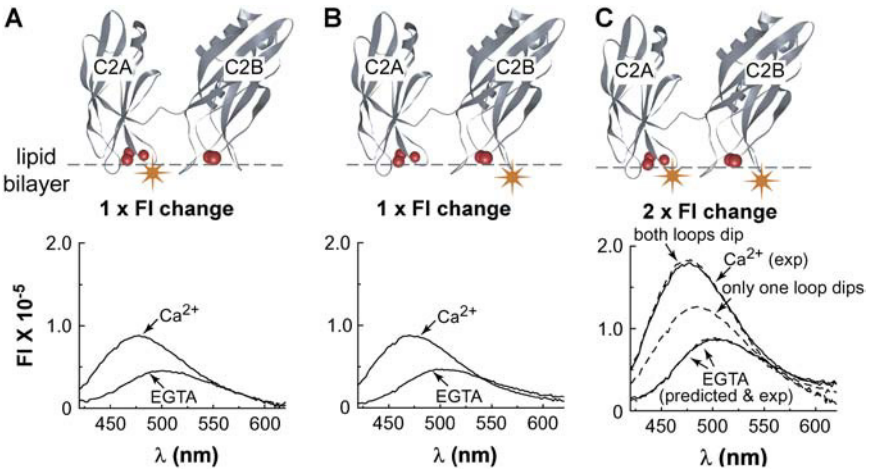

FIGURE 1 In context of C2A-C2B, Ca^{2+}/liposome-triggered fluorescence changes of C2A and C2B are additive. For all experiments shown in this figure, synthetic phospholipids and the intact cytoplasmic domain of syt (C2A-C2B) were used. FI is abbreviation for fluorescence intensity. (*A*) Upper panel, molecular model depicting the penetration of C2A(3) (Ca^{2+}-binding loop 3 of C2A) into PS-harboring lipid bilayers. The site-directed fluorescent probe, AEDANS, is shown as an orange star. The solution structures of C2A and C2B were rendered using WebLab Viewer Lite (Molecular Simulations, San Diego, CA); the linker that connects them was added using a drawing program. Ca^{2+} ions are shown as red spheres. Lower panel, the fluorophore on C2A(3) exhibited a Ca^{2+}-triggered increase in fluorescence intensity and a blue-shift in the emission spectrum when mixed with PS/PC liposomes. (*B*) Upper panel, molecular model depicting the penetration of C2B(3) (Ca^{2+}-binding loop 3 of C2B) into PS-harboring lipid bilayers. Lower panel, the fluorophore on C2B also exhibited a Ca^{2+}-triggered increase in intensity and a blue-shift in the emission spectrum when mixed with PS/PC liposomes. (*C*) Upper panel, molecular model depicting the penetration of both C2A(3) and C2B(3) into PS-harboring lipid bilayers. Lower panel, the double-labeled cytoplasmic domain of syt, C2A*(3)-C2B*(3), exhibited a twofold larger Ca^{2+}-triggered increase in fluorescence intensity than the single-labeled proteins in panels *A* and *B* and a blue-shift in the emission spectrum when mixed with liposomes that harbor PS (shown as *solid lines*). The dashed lines represent the predicted spectra that were calculated from the spectra of the two single-labeled mutants from panels *A* and *B*. The bottom and top dashed lines were calculated by adding the spectra from panels *A* and *B* together, before and after the addition of Ca^{2+}, respectively. The top solid line, which represents the fluorescence spectrum of C2A*(3)-C2B*(3) after the addition of Ca^{2+} and liposomes, agreed very well with the top dashed line. Thus, the results shown here are consistent with a model in which C2A and C2B copenetrate PS-containing bilayers in response to Ca^{2+}.

Moreover, we generated a double-labeled Cys mutant—C2A*(3)-C2B*(3)—in which loop 3 of both C2A and C2B are labeled (Fig. 1 *C*, *upper panel*). If both C2A and C2B insert into PS/PC membranes, the fluorescence change in C2A*(3)-C2B*(3) would be the sum of the changes exhibited by C2A*(3)-C2B and C2A-C2B*(3). As shown in Fig. 1 *C* (*lower panel*), this was in fact the case—the fluorescence changes exhibited by the double-labeled mutant corresponded to the sum of the signals from the individually labeled C2-domains. The solid lines, which were obtained from fluorescence measurements of C2A*(3)-C2B*(3), agree very well with the corresponding dashed lines that were calculated by summing the spectra of the two single (C2A*(3)-C2B and C2A-C2B*(3)) labeled proteins. The additive Ca^{2+}/liposome-induced changes in the fluorescence signals from C2A and C2B are consistent with a model in which the tandem C2-domains of syt copenetrate into the hydrophobic core of lipid bilayers.

The findings described above could also be explained by another model: the C2A and C2B penetrate into the lipid bilayer in an equal, yet mutually exclusive, manner. For example, we consider the possibility that, among a population of C2A-C2B molecules, only C2A interacts with membranes in half the population whereas only C2B interacts with membranes in the other half of the population at any given time (Fig. 2 *A*, *lower panel*). In this case, the fluorescence change of each singly labeled C2A-C2B corresponds to penetration of only half of the C2A-C2B molecules into the bilayer. Thus, the fluorescence increase of double-labeled C2A-C2B would also be ~2-fold. This possibility was ruled out by comparing the fluorescence spectra of C2A*(3)-C2B and C2A*(3)-$C2B_M$; this latter construct is a mutant in which the membrane penetration activity within C2B has been completely disrupted (14). This construct was selected for two reasons: first, C2A has been shown to penetrate membranes with a nanomolar affinity ($k_{on} \gg k_{off}$) (10) and efficiently cosediments with liposomes under conditions similar to the fluorescence measurements reported here (please refer to Fig. 5 *A*). These data indicate that most, if not all, of the C2A-$C2B_M$ molecules absorb onto liposomes in response to Ca^{2+}. Second, the mutant C2B domain of C2A*(3)-$C2B_M$ does not penetrate membranes and thus is unable to compete with C2A. Hence, in C2A*(3)-$C2B_M$, virtually all of the Ca^{2+}/membrane-binding loops of C2A are expected to be buried into the membrane (Fig. 2 *B*, *lower panel*). If the membrane penetration activity of C2A and C2B are mutually exclusive (that is, they ''compete'' with each other for insertion into bilayers), we would expect to see a larger fluorescence change (upon inserting into bilayers) in C2A*(3)-$C2B_M$ than in C2A*(3)-C2B. However, disruption of the membrane penetration activity of C2B failed to increase the penetration of C2A, demonstrating that C2A and C2B, within the cytoplasmic domain of syt, do not penetrate membranes in a mutually exclusive manner. We conclude that C2A and C2B copenetrate membranes.

As alluded to above, the spectral changes observed in Figs. 1 and 2 have been previously shown, using membrane-embedded quenchers and the parallax method, to be due to direct penetration of the AEDANS reporter (on loop 3) into the hydrophobic core of lipid bilayers (32). We have extended these experiments to include AEDANS probes on loop 1 of C2A or C2B and found that these Ca^{2+}-binding loops penetrate membrane in a manner analogous to loop 3 (~1/5th into the hydrophobic core of the PS/PC bilayer; Supplementary Fig. 1). These experiments confirm that Ca^{2+}-binding loops 1 and 3, in both C2-domains, penetrate PS/PC membranes in response to Ca^{2+}.

We next determined whether C2A and C2B penetrate membranes simultaneously or with distinct kinetics, using a stopped-flow rapid mixing approach. Rapid mixing of liposomes and Ca^{2+} with C2A*(3)-C2B, C2A-C2B*(3), or C2A*(3)-C2B*(3) resulted in rapid changes in all three fluorescence signals (Fig. 3 *A*). The raw data traces were well fitted with single exponential functions. Using 11 nM liposomes (100 nm in diameter), the observed rates (k_{obs}) were 228 s^{-1}, 230 s^{-1}, and 205 s^{-1} for C2A*(3)-C2B, C2A-C2B* (3) and C2A*(3)-C2B*(3), respectively. We then measured k_{obs} as a function of [liposome] and calculated the on-rate (k_{on}), off-rate (k_{off}), and the dissociation constants (K_d) for labeled C2A-C2B-liposome interactions as described in Fig. 3 *D*; these data are summarized in Fig. 3 *E*. Consistent with previous reports using brain-derived phospholipids (32), the on-rates for C2A*(3)-C2B and C2A-C2B*(3) penetration are almost identical and both approach the diffusion limit. Moreover, the fluorescence changes for double-labeled C2A*(3)-C2B*(3) were also well fitted by single exponential functions, further supporting the idea that C2A and C2B copenetrate membranes simultaneously, or at least within the uncertainty of the kinetics measurements. We note that the double-labeled protein, C2A*(3)-C2B*(3) exhibited a slightly lower on-rate and a slightly higher off-rate than the mutants with only a single label. These subtle changes could be due to the AEDANS label, which is a bulky molecule (~12 Å) that carries a negative charge. However, parallel experiments using FRET to monitor protein-lipid interactions (using wild-type C2A-C2B lacking a label) revealed that the AEDANS probe had little, if any, effect on the kinetics of C2A-C2B-membrane interactions (Fig. 6 *B* compared to Fig. 3 *E*).

In the next series of experiments, we sought to shed light on the debate regarding the ability of isolated C2B to interact with PS-bearing membranes (20,32,34). Although it is well established that C2B interacts with PS/PC membranes in the context of C2A-C2B, it is unclear whether the isolated C2B domain binds PS-containing membranes with high affinity. In some studies, low or trace levels of binding were reported (14,20,32,33). However, in another study it was reported that isolated C2B penetrated PS/PC membranes as well as C2A (34).

To address this apparent contradiction, we explored the stability of the putative membrane penetration activity of

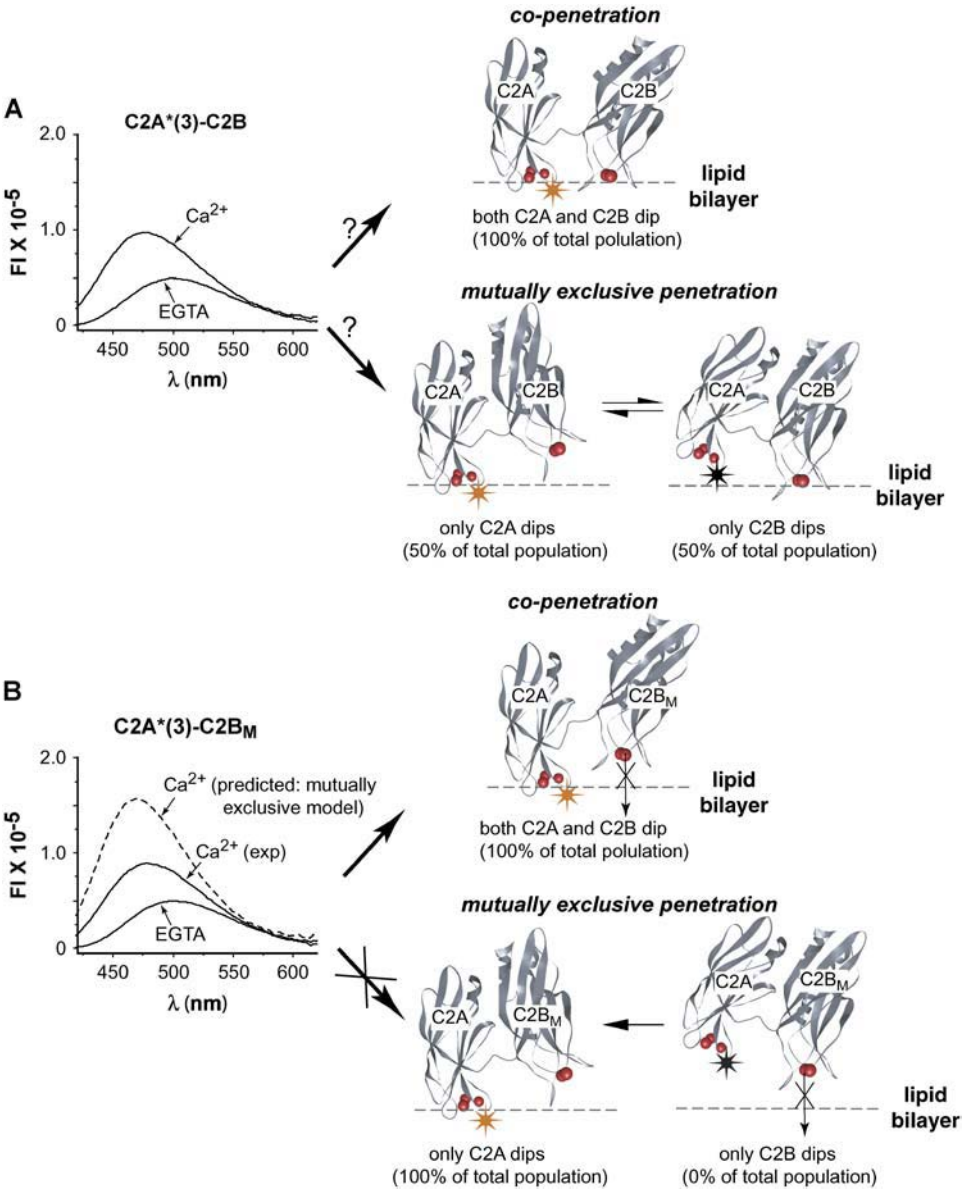

FIGURE 2 C2A and C2B do not penetrate membranes in a mutually exclusive manner. All symbols shown in this figure are the same as in Fig. 1 except that the AEDANS label is shown as a black star when it is not inserted into the membrane. (*A*) The fluorescence data shown in Fig. 1 are consistent with two distinct models. A graphic representation of single-labeled protein, C2A*(3)-C2B, is used to illustrate these two different models. Upper right panel, copenetration model in which both C2-domains of C2A-C2B dip into membranes in response to Ca^{2+}. Lower right panel, exclusive penetration model in which C2A and C2B dip into the lipid bilayer in an equal, yet mutually exclusive, manner. For example, we consider the possibility that, among a population of C2A-C2B molecules, only C2A interacts with membranes in half the population whereas only C2B interacts with membranes in the other half of the population at any given time. In this case, the fluorescence change of C2A*(3)-C2B corresponds to penetration of C2A domain of only half the population of the C2A*(3)-C2B molecules into the bilayer. Left panel, the experiment in Fig. 1 *A* was repeated. Penetration of the AEDANS label of C2A*(3)-C2B into membranes resulted in an increase (90%) in the fluorescence intensity (FI). These Ca^{2+}/liposome-triggered spectral changes in C2A*(3)-C2B can be explained by either of the two models. Similarly, data shown in Fig. 1, *B* and *C* (omitted here) could also be explained by either model in the right panels. (*B*) Inactivation of C2B domain within C2A-C2B does not enhance the membrane penetration of C2A. We used a mutant protein, C2A*(3)-$C2B_M$, in which the membrane penetration activity of C2B was abolished via Ca^{2+} ligand mutations as described in Materials and Methods. Upper right panel, in the copenetration model, inactivation of C2B is expected to have little effect on the penetration of C2A. Lower right panel, in the exclusive penetration model, inactivation of C2B is expected to convert the total population of C2A-C2B molecules into one state in which only C2A dips into the membrane. In this scenario, the Ca^{2+}/liposome-triggered fluorescence increase exhibited by C2A*(3)-$C2B_M$ would be roughly twice that of C2A*(3)-C2B. Given that the FI increased by 90% for C2A*(3)-C2B, this model predicts an increase for 180% for the FI of C2A*(3)-$C2B_M$. Left panel, the experiment in Fig. 2 *A* was repeated, but using the construct C2A*(3)-$C2B_M$. The predicted spectrum (*dashed line*) upon addition of Ca^{2+} is calculated according to the exclusive penetration model as illustrated in the lower right panel. The experimentally observed increase in FI upon penetration of the probe in C2A into the bilayer was 73%, which does not agree with the prediction from the mutually exclusive penetration model. Hence, the tandem C2-domains do not penetrate in a mutually exclusive manner but rather copenetrate into the bilayer.

isolated C2B using the AEDANS probes described above. The degree of penetration was assayed as a function of ionic strength. Ca^{2+}/liposome-dependent fluorescence changes of the AEDANS probe in isolated C2B*(3), C2A-C2B*(3), and $C2A_M$-C2B*(3) were compared (Fig. 4). We found that isolated C2B*(3) exhibited only low levels of membrane penetration activity in the presence of 100 mM NaCl. However, this interaction was extremely sensitive to ionic strength, as evidenced by the sharp decrease in the degree of penetration as the [NaCl] was increased to physiological concentrations (Fig. 4 *D*).

In these experiments, the membrane penetration activity of loop 3 of isolated C2B was abolished by 150 mM NaCl. However, an adjacent C2A domain strongly enhanced the membrane penetration activity of C2B (Fig. 4 *B*). This penetration activity was not dependent on the Ca^{2+}-binding ability of C2A, since C2B could also be activated by a

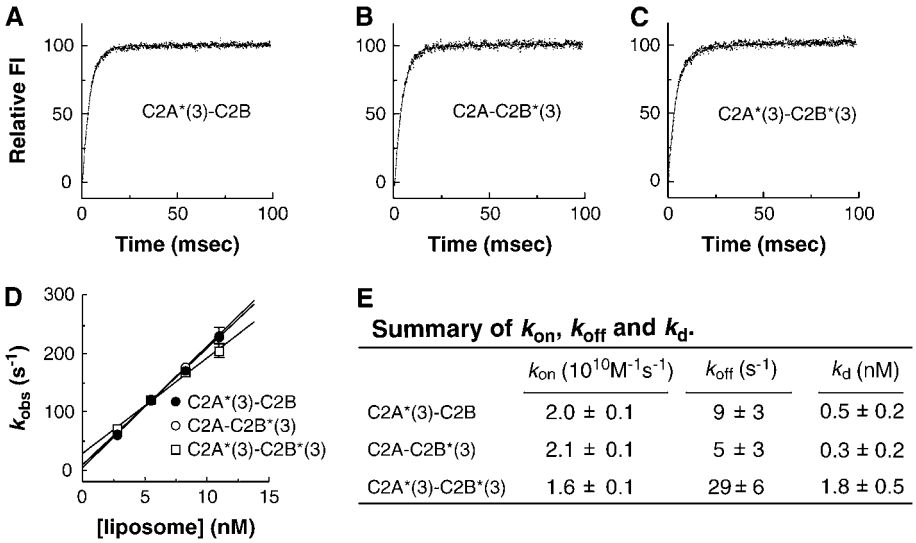

E

Summary of k_{on}, k_{off} and k_d.

	k_{on} ($10^{10}M^{-1}s^{-1}$)	k_{off} (s^{-1})	k_d (nM)
C2A*(3)-C2B	2.0 ± 0.1	9 ± 3	0.5 ± 0.2
C2A-C2B*(3)	2.1 ± 0.1	5 ± 3	0.3 ± 0.2
C2A*(3)-C2B*(3)	1.6 ± 0.1	29 ± 6	1.8 ± 0.5

FIGURE 3 In the context of C2A-C2B, C2A and C2B copenetrate PS/PC bilayers with rapid and indistinguishable kinetics. The cytoplasmic domain of syt (C2A-C2B) was labeled as described in Fig. 1 *A*, and stopped-flow rapid mixing experiments were carried out as described in Materials and Methods. (*A*) C2A*(3)-C2B (1 μM) was premixed with 22 nM liposomes (2 mM total phospholipids) in the presence of EGTA (0.1 mM) and then rapidly mixed with Ca^{2+} (0.5 mM final free [Ca^{2+}]). The raw data traces can be well fitted with a single exponential function (k_{obs} = 228 s^{-1}). (*B*) The same experiment was carried out except using C2A-C2B*(3) (k_{obs} = 230 s^{-1}). (*C*) The same experiment was carried out except using double-labeled protein C2A*(3)-C2B*(3) (k_{obs} = 205 s^{-1}). In this last case, the data traces can also be well fitted by single exponential functions, suggesting that C2A and C2B simultaneously copenetrate membranes. (*D*) To determine k_{on} and k_{off} for these binding interactions, k_{obs} was plotted as a function of [liposome]. The *Y* intercept yields k_{off}, and the slope yields k_{on} for the interaction of C2A-C2B with membranes in the presence of Ca^{2+}. Error bars represent the standard deviation from three independent experiments. The dissociation constants (K_d) for C2A-C2B-liposome interactions, in the presence of Ca^{2+}, were calculated as k_{off}/k_{on}. (*E*) Summary of the K_d, k_{on}, and k_{off} values obtained from panel *D*. The AEDANS reporters in C2A*(3)-C2B and C2A-C2B*(3) penetrate membranes composed of synthetic PS/PC with similar kinetics, in agreement with previous results using liposomes composed of brain-derived PS/PC (32).

''dead'' C2A domain (designated $C2A_M$; Fig. 4 *C*) that does not bind membranes or Ca^{2+} (32). A significant degree of membrane penetration of loop 3 of C2B, in the context of $C2A_M$-C2B, persisted at very high salt concentrations, indicating that this is a highly stable interaction (Fig. 4 *D*). These data agree with our previous model in which C2A activates an otherwise hidden or cryptic membrane penetration activity within the adjacent C2B domain.

Changes in ionic strength can affect the emission spectra of a number of fluorophores. In this study, increasing the ionic strength caused only a minor decrease in the fluorescence intensity of AEDANS-labeled C2A-C2B free in solution (Supplementary Fig. 2). Therefore, the marked decrease in fluorescence intensity that we observed in Fig. 4 *D* is mainly due to loss of membrane penetration activity.

Brain-derived phospholipids were used in our previous studies in which isolated C2B failed to penetrate membranes (32), whereas synthetic phospholipids were used by Rufener et al. (34) who reported efficient membrane penetration activity of isolated C2B. Here, both types of phospholipids were used and compared. The level of C2B*(3) penetration was somewhat greater using synthetic phospholipids, but this did not change the overall trend in these experiments, further supporting a model in which C2A activates a cryptic membrane penetration activity within C2B (32). It is not clear why native and synthetic lipids yield somewhat different results. Possible reasons include differences in acyl chain packing and bilayer fluidity. Alternatively, these differences might rise from oxidative damage of the natural lipids, owing to the instability of polyunsaturated acyl chains or from the presence of impurities that quench the fluorophore or alter the properties of the bilayer.

For comparison, AEDANS was also used to explore the penetration activity of loop 1 of C2B, both in the context of isolated C2B (Supplementary Fig. 3 *B*) and in the intact cytoplasmic domain of syt, C2A-C2B (Supplementary Fig. 1 *C*). In isolated C2B, loop 1 was able to penetrate membranes to some degree at physiological salt concentrations. This activity was weaker than the positive control, isolated C2A, but was stronger than the penetration activity of loop 3 of C2B (Supplementary Fig. 3, *A* and *D*). The interaction between loop 1 of C2B and PS/PC membranes was readily disrupted by increasing the ionic strength, especially when the liposomes were generated from brain-derived phospholipids (Supplementary Fig. 3, *B* and *D*). Again, the stability was greatly enhanced by an adjacent C2A domain (Supplementary Fig. 3, *C* and *D*).

Direct comparison between the penetration of C2A-C2B*(1) and C2A-C2B*(3) revealed some interesting differences. In the context of C2A-C2B, at low salt concentrations, loop 3 of C2B penetrated more efficiently into the membrane than loop 1 (Fig. 4 *D* compared to Supplementary Fig. 3 *D*). However, the penetration of loop 1 was more stable, as evidenced by its greater resistance to increasing ionic strength. These results suggest that the two Ca^{2+}-binding loops within the C2B domain are not equal. In light of these findings, we compared the penetration kinetics of loops 1 and 3 of C2B, again in the context of C2A-C2B, using a stopped-flow rapid mixing approach. Labels in either loop of C2B reported similar penetration kinetics (Supplementary Fig. 3, *E–G*). The observed rate constant for C2A-C2B* (1) was only slightly less than that of C2A-C2B* (3). It is likely that in response to Ca^{2+}, both loops of C2B rapidly dip into the membrane. However, the

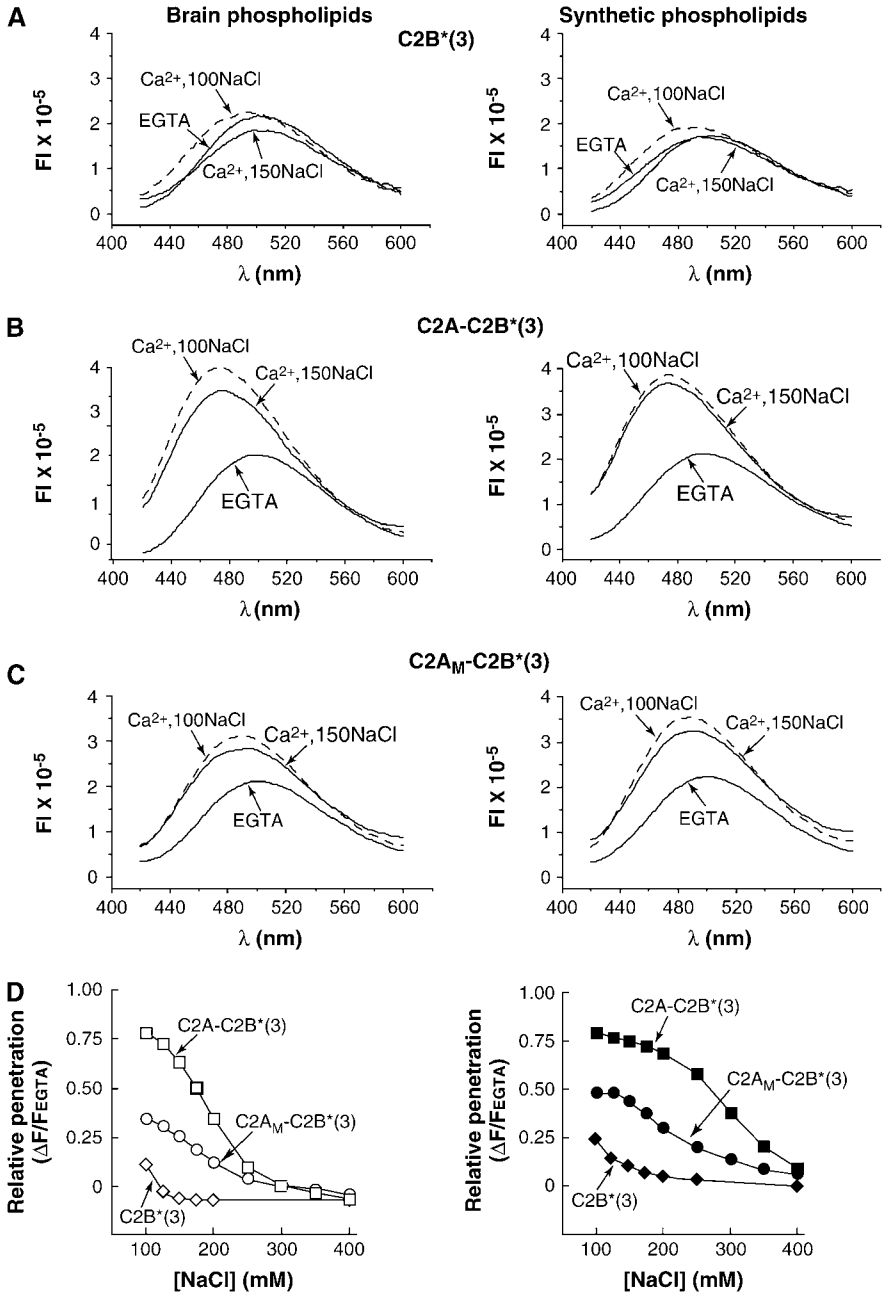

FIGURE 4 An adjacent C2A-domain activates the membrane penetration in loop 3 of the C2B domain of syb I. Ca^{2+}/liposome-induced changes in the fluorescence of isolated C2B*(3), C2A-C2B*(3), and $C2A_M$-C2B*(3) were compared. Each protein was adjusted to 0.5 μM in HEPES buffer and excited at 336 nm; the emission spectra were collected from 420 to 600 nm. Liposome composition (25% PS/75% PC) and concentration (11 nM liposomes or 1 mM total lipids) were the same for all experiments unless otherwise indicated. Fluorescence spectra, obtained using liposomes composed of brain-derived PS/PC (*left panels*) or synthetic PS/PC (*right panels*), were compared side by side. Spectra were first obtained in the presence of 0.1 mM EGTA and liposomes. Ca^{2+} was then added to a final free concentration of 0.5 mM, and the emission spectra were collected again. NaCl was added afterward to elevate [NaCl] to 125, 150, 175, 200, 250, 300, 350, and 400 mM, and the emission spectra at each [NaCl] were collected. (*A*) The emission spectra of isolated C2B*(3) in the presence of liposomes. Only three representative spectra are shown: EGTA at 100 mM NaCl (*solid line*), Ca^{2+} at 100 mM NaCl (*dashed line*), and Ca^{2+} at 150 mM NaCl (*solid line*), as indicated in the figure. (*B*) The emission spectra of C2A-C2B*(3) and (*C*) the emission spectra of $C2A_M$-C2B* (3) were obtained as described in panel *A*. (*D*) Quantification of the ''penetration spectra''. Each emission spectrum was integrated, and the area under the spectrum in the presence of EGTA (designated F_{EGTA}) was subtracted from spectrum obtained in the presence of Ca^{2+} (designated F^{2+}_{Ca}), yielding the difference ΔF ($= F^{2+}_{Ca} - F_{EGTA}$), which was subsequently divided by F_{EGTA}. The quotient $\Delta F/F_{EGTA}$ served as an indicator of membrane penetration in response to Ca^{2+} (20); these values were plotted as a function of [NaCl].

interaction of loop 1 with PS/PC membranes seems to be stronger or at least less dependent on electrostatic interactions than that of loop 3. This latter possibility is supported by the presence of two lysine residues (K-366 and K-369) within loop 3 of C2B and the absence of charged residues in loop 1 of C2B.

To further characterize the effects of ionic strength on the interaction of syt with liposomes, we carried out C2A-C2B-liposome cosedimentation assays. Cosedimentation, using isolated or tethered C2-domains, was monitored as a function of ionic strength (Fig. 5 *A*). In all cases, cosedimentation was sensitive to ionic strength, consistent with previous reports (36,40). The positive control, wild-type C2A-C2B, exhibited the greatest salt resistance, whereas the isolated C2B domain was readily stripped from liposomes by increasing the ionic strength. However, when a mutant C2A ($C2A_M$) domain that fails to bind Ca^{2+} or PS (32) was tethered to C2B, resistance to increasing ionic strength was greatly enhanced, indicating a significant increase in the strength and/or stability of the protein-membrane complexes. In addition, experiments utilizing isolated C2-domains revealed that Ca^{2+}·C2A-membrane complexes were much more resistant to high salt than Ca^{2+}·C2B·membrane complexes. C2A·membrane interactions were also slightly enhanced by an adjacent mutant C2B domain ($C2B_M$) that fails to bind Ca^{2+} or PS, but this enhancement was much weaker than that of $C2A_M$ on C2B. In

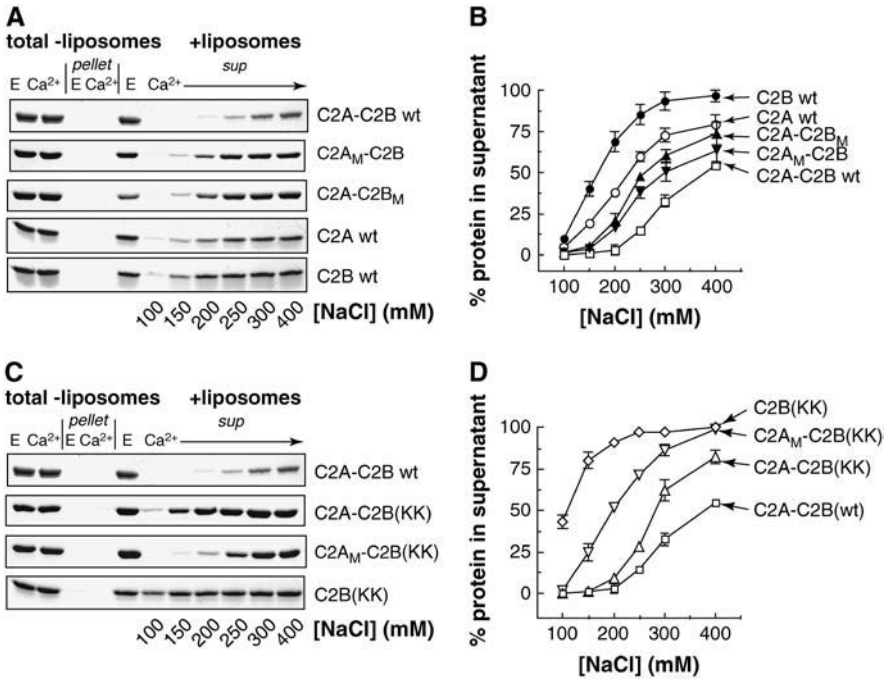

FIGURE 5 Effect of ionic strength on the cosedimentation of Ca^{2+}-syt with liposomes. (*A*) The sensitivity of Ca^{2+}·syt·PS/PC liposome interactions to ionic strength was studied using a cosedimentation assay as described previously (36), using different syt fragments as indicated. In the absence of liposomes, sedimentation was not observed in either EGTA or Ca^{2+}. In the presence of liposomes, sedimentation did not occur in EGTA but was triggered by Ca^{2+}. Sedimentation in the presence of Ca^{2+} was assayed at increasing concentrations of NaCl; identical fractions of the supernatant from each sample were loaded onto the gel. With increasing [NaCl], wild-type C2A-C2B, C2A, C2B, and the indicated mutant C2A-C2B fragments were stripped from the pellet and recovered in the supernatant fraction. (*B*) Quantification of the effect of [NaCl] on the cosedimentation of Ca^{2+}-syt with PS/PC liposomes. The Coomassie-stained gels from panel *A* were quantified using an Epi Chemi II Darkroom gel documentation system and Labworks 4.0 software (UVP Bio-Imaging Systems, Upland, CA); percent recovery of protein in the supernatant was plotted as a function of [NaCl]. (*C*) Effects of lysine substitutions (K-326, 327A, designated KK), which diminish cosedimentation by abolishing oligomerization of syt (33), on the sensitivity of cosedimentation as a function of ionic strength. Wild-type C2A-C2B was used as the positive control. With increasing [NaCl], the indicated KK mutant fragments of syt were stripped from the pellet and recovered in the supernatant fraction. (*D*) Quantification of the effect of [NaCl] on the cosedimentation of syt fragments from panel *C*.

terms of binding PS, C2A has a more significant effect on C2B than vice versa.

Since sedimentation involves both the membrane binding and oligomerization activity of syt fragments (33), the differences described above could be due to differences in either, or both, of these interactions. Therefore, we generated and purified K-326, 327A (designated KK) mutant versions of the syt fragments, which have been shown to lack oligomerization activity but have normal PS-binding activity (33). In 100 mM NaCl, the KK mutation reduced the sedimentation activity of C2B by ~60%; the remaining sedimentation is likely to represent the contribution from the relatively weak membrane-binding activity of C2B. This residual sedimentation activity was largely abolished when the salt concentration was increased to physiological levels (Fig. 5, *C* and *D*). These findings further indicate that the isolated C2B domain of syt does not avidly bind to PS (33). The presence of an adjacent C2A markedly enhanced the membrane-binding activity of C2B. Notably, this enhancement is not due to the ability of C2A to bind membranes and thereby ''drag'' the adjacent C2B domain onto membranes, since a ''dead'' C2A ($C2A_M$) also enhanced the interaction to a significant extent. These results again confirm that C2A affects the properties of C2B.

The inability of isolated C2B to avidly interact with PS/PC membranes could be due to the presence of an N-terminal sequence that is not actually part of the structure of C2B. Structural data indicate that C2B actually begins at or near residue 271 (14,45). The experiments reported in this study made use of a construct that began at residue 248 because this longer construct is more readily purified in a soluble form. We compared the properties of the larger C2B construct (residues 248–421) with the shortest possible construct that did not contain any additional flanking residues (residues 271–421). These two versions of C2B exhibited identical abilities to cosediment with PS/PC liposomes as a function of increasing ionic strength (Supplementary Fig. 4). These data indicate that the longer C2B construct is not self-inhibited by the presence of extra residues at the N-terminus.

In all of the experiments reported in this study, ''clean'' fragments of syt, in which all bacterial contaminants had been removed (14,33), were used. We have also characterized ''dirty'' C2B that carries the bacterial contaminants (which are RNA and/or DNA) and found no significant differences in the fluorescence and cosedimentation experiments (E. Hui and E. R. Chapman, unpublished observations).

The kinetics of Ca^{2+}-triggered membrane penetration of C2A has been studied in detail (10), but little is known concerning the kinetics of C2B. In the final series of experiments we measured the kinetics of C2B·membrane interactions. Since isolated C2B exhibits little PS-binding activity, we carried out these experiments using $C2A_M$-C2B. In this construct, $C2A_M$ cannot bind Ca^{2+} or PS but can enhance the PS penetration activity of the adjacent C2B domain (Fig. 4 *D* and Bai et al. (32)), making it possible to measure the kinetics of Ca^{2+}-C2B-PS interactions. For these experiments we monitored protein·liposome complex formation using FRET from the native tryptophan residues in $C2A_M$-C2B to a

dansyl-acceptor (attached to the headgroup of phosphatidylethanolamine (PE)) on the liposomes. Stopped-flow rapid mixing experiments were carried out as a function of [liposome] as described in Fig. 3. These experiments indicate that C2B-mediated interactions with PS/PC liposomes occur on rapid timescales and approach the collision limit for complex assembly (Fig. 6, *A* and *B*). Like C2A, C2B rapidly senses Ca^{2+} and binds to membranes, readily fulfilling the kinetic constraints of rapid exocytosis.

DISCUSSION

Initial biochemical studies of syt revealed that this synaptic vesicle protein binds to PS-bearing membranes in response to Ca^{2+} (46). These results suggested that syt might function as a Ca^{2+} sensor during neuronal exocytosis, and this idea was confirmed in numerous biochemical, genetic, and biophysical experiments (4–6,24). However, the molecular mechanism by which Ca^{2+} and syt regulate membrane fusion is not yet understood. It was recently shown that PS is an essential effector for the action of Ca^{2+}·syt in the regulation of SNARE-catalyzed membrane fusion that had been reconstituted in vitro (26,31). Hence, the mechanism by which Ca^{2+}·syt engages anionic phospholipids is critical for our understanding of the mechanism of regulated membrane fusion. Previous studies demonstrated that upon binding Ca^{2+}, the C2-domains of the cytoplasmic domain of syt (C2A-C2B) partially penetrate into PS/PC membranes. However, it was not clear whether C2A and C2B penetrate bilayers simultaneously or whether the tandem C2-domains penetrate into membranes in a mutually exclusive manner.

Combining site-directed fluorescent probes and a stopped-flow rapid mixing approach, we found that in response to Ca^{2+}, the Ca^{2+}-binding loops of both C2A and C2B simultaneously dip into PS/PC bilayers with rapid and apparently identical kinetics. These experiments demonstrate that when Ca^{2+}·syt engages PS, Ca^{2+}-binding loops of both C2-domains simultaneously insert into the PS-harboring membrane. However, disruption of the Ca^{2+} and PS-binding activity of either C2A or C2B had surprisingly mild effects on the dissociation constant (K_d) or off-rate of C2A-C2B·liposome complexes (Fig. 6 *B*). It has been shown that, in some cases, tethering two independent domains together can greatly enhance the overall affinity of binding between macromolecules since binding of one domain increases the local concentration of the other and vice versa (47). Disruption of the Ca^{2+}- and membrane-binding activity of either C2-domain of syt would eliminate this enhancement and give rise to significant effects on the off-rate and K_d for syt·membrane interactions. These changes, however, were not observed in our study (Fig. 6 *B*). Thus, a likely explanation for these results is that C2A and C2B synergize in a complex manner to bind to membranes and are not completely autonomous domains connected by a linker.

The complexity of the synergistic relationship between C2A and C2B is further illustrated by comparisons between the PS-binding properties of the isolated C2-domains of syt. In this study, cosedimentation assays and fluorescent probes were applied to examine C2B·membrane interactions under various conditions. In both assays, the interaction between the C2B domain of syt and membranes composed of PS/PC was generally much weaker and less resistant to salt when compared to C2A and C2A-C2B. When C2B was tethered to $C2A_M$, which is a mutant version of C2A that is unable to bind Ca^{2+} or PS/PC membranes (as demonstrated in Bai et al. (32)), the stability of the protein-membrane complex was markedly enhanced. These data confirm that a novel form of synergy or cooperativity between C2A and C2B (rather than the Ca^{2+}-dependent membrane-binding activity of C2A) converts the C2B domain into a high affinity membrane-binding module (32). In addition, two Ca^{2+}-binding loops of C2B also exhibit different abilities to penetrate into PS/PC bilayers; i.e., in response to Ca^{2+}, Ca^{2+}-binding loop 1, but not loop 3, dips into PS/PC membranes even in buffers with relatively high ionic strength. This may be due to the fact that there are two lysine residues located in loop 1 but only neutral residues are present in loop 3. However, the overall interaction of unlabeled isolated C2B with PS/PC liposomes

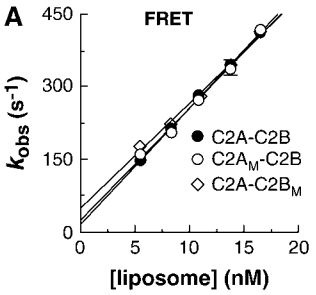

B Summary of k_{on}, k_{off} and K_d.

	k_{on} ($10^{10}M^{-1}s^{-1}$)	k_{off} (s^{-1})	K_d (nM)
C2A-C2B	2.4 ± 0.2	16 ± 8	0.7 ± 0.4
$C2A_M$-C2B	2.3 ± 0.2	25 ± 19	1.2 ± 0.9
C2A-$C2B_M$	2.2 ± 0.2	49 ± 26	2.4 ± 1.4

FIGURE 6 Kinetics of the C2B-domain of syt. (*A*) FRET between the native tryptophan residues in C2A-C2B and a dansyl-PE acceptor was used to monitor binding to PS/PC liposomes using a stopped-flow rapid mixing approach. Wild-type C2A-C2B (*solid circles*) and mutant versions in which membrane-binding activity was selectively disrupted in either the C2A (D-230, 232N; designated $C2A_M$-C2B, *open circles*) or C2B-domains (D-363, 365N; designated C2A-$C2B_M$, *open diamonds*) were compared. Protein plus 0.5 mM Ca^{2+} was rapidly mixed with the indicated [liposome] in a stopped-flow spectrometer. The increase in fluorescence of the acceptor was well fitted with a single exponential function to yield k_{obs}, and k_{obs} was plotted versus [liposome]. From these data, the on-rate (k_{on}) and off-rate (k_{off}) were obtained, and the dissociation constants (K_d) were calculated as described in Fig. 3 *D*. (*B*) Summary of rate and dissociation constants. Disruption of C2A or C2B reduced the affinity ~1.6- and ~3.3-fold respectively; however, nM affinity binding was preserved in both mutants. In $C2A_M$-C2B, all PS-binding activity is mediated by the C2B domain and data obtained with this construct report the kinetics of this domain; this analysis indicates that C2B has similar kinetics to the C2A-domain and fulfills the kinetics constraints of rapid exocytosis.

is more sensitive to ionic strength than isolated C2A, $C2A_M$-C2B, and C2A-C2B in the cosedimentation assay (Fig. 5). According to this assay, Ca^{2+}·C2B·PS/PC interactions are relatively weak, as C2B can be readily stripped from PS/PC vesicles at moderate ionic strength.

The data reported here highlight the idea that the properties of the C2B domain of syt can be profoundly influenced by the adjacent C2A domain. Our data also reveal that some of the uncertainty regarding the interaction of isolated C2B with PS/PC membranes can be largely attributed to differences in ionic strength of the buffers, the use of different kinds of binding assays (e.g., FRET/stopped-flow, fluorescent probe penetration, cosedimentation, etc.), and differences in materials (e.g., synthetic versus natural phospholipids). In particular, Rufener et al. reported that isolated C2A and C2B bind PS/PC membranes with a similar affinity and that isolated C2B dips into PS/PC bilayers in a manner that is very similar to C2A (34). However, in their study, the affinity of the C2B-membrane interaction was measured using Tb^{3+} and not Ca^{2+}.

We have found that Ca^{2+} is unable to effectively compete with Tb^{3+} for binding to C2-domains (L. F. Davis and E. R. Chapman, unpublished observations). Thus, Tb^{3+} might not mimic the effects of Ca^{2+} in terms of activating syt-membrane interactions. For membrane dipping, electron spin resonance experiments were carried out using high concentrations of protein and lipid (20–300 μM isolated C2B and 40–60 mM lipids) as compared to our fluorescence assays (0.5 μM C2B and 1 mM total lipids). High concentrations of protein would favor binding despite the low affinity of Ca^{2+}-C2B-membrane complexes. Finally, Rufener et al. used synthetic, rather than natural, phospholipids. As we show in this study, isolated C2B is more likely to penetrate membranes made with synthetic phospholipids. The emerging view is that isolated C2B binds to PS/PC membranes much more weakly than C2A, but under some conditions, isolated C2B can partially penetrate into PS/PC bilayers.

The main finding reported here is that in the intact cytoplasmic domain of syt, C2A and C2B rapidly copenetrate into PS/PC bilayers; both Ca^{2+}-binding loops 1 and 3, in both C2-domains, penetrate into the hydrophobic core of membranes. Hence, a detailed view of the dynamics of Ca^{2+}·syt-membrane interactions, and the structure of this complex, has emerged (10,12,13,20,32,34,48). The interaction of syt with lipid bilayers can drive the close apposition of membranes (49,50) to potentially facilitate membrane fusion (20,31,46). Also, it was recently shown that the interaction of syt with PS facilitates the assembly of SNARE complexes, which may also serve to trigger membrane fusion (26).

A number of studies indicate that both C2-domains of syt play roles in the regulation of exocytosis and membrane fusion (e.g., 21,24,31,35,36,51–54). The precise mechanisms by which syt regulates secretion will be further revealed by addressing the immediate consequences of Ca^{2+} binding to its tandem C2-domains. New insights will be gained by studying the behavior of single molecules, by increasing the time resolution of dynamic measurements, and by studying rearrangements between syt and its effectors in living cells.

SUPPLEMENTARY MATERIAL

An online supplement to this article can be found by visiting BJ Online at http://www.biophysj.org.

We thank Meyer Jackson and members of the Chapman lab for discussions and comments.

This study was supported by grants from the National Institutes of Health (NIGMS GM 56827 and NIMH MH61876) and the American Heart Association (0440168N) to E.R.C.. E.R.C. is an Investigator of the Howard Hughes Medical Institute.

REFERENCES

1. Katz, B. 1969. The Release of Neural Transmitter Substances. Thomas, Springfield, IL.
2. Meinrenken, C. J., J. G. Borst, and B. Sakmann. 2003. Local routes revisited: the space and time dependence of the Ca^{2+} signal for phasic transmitter release at the rat calyx of Held. *J. Physiol.* 547:665–689.
3. Schneggenburger, R., and E. Neher. 2005. Presynaptic calcium and control of vesicle fusion. *Curr. Opin. Neurobiol.* 15:266–274.
4. Augustine, G. J. 2001. How does calcium trigger neurotransmitter release? *Curr. Opin. Neurobiol.* 11:320–326.
5. Koh, T. W., and H. J. Bellen. 2003. Synaptotagmin I, a Ca^{2+} sensor for neurotransmitter release. *Trends Neurosci.* 26:413–422.
6. Chapman, E. R. 2002. Synaptotagmin: a Ca^{2+} sensor that triggers exocytosis? *Nat. Rev. Mol. Cell Biol.* 3:498–508.
7. Perin, M. S., V. A. Fried, G. A. Mignery, R. Jahn, and T. C. Sudhof. 1990. Phospholipid binding by a synaptic vesicle protein homologous to the regulatory region of protein kinase C. *Nature.* 345:260–263.
8. Perin, M. S., N. Brose, R. Jahn, and T. C. Sudhof. 1991. Domain structure of synaptotagmin (p65). *J. Biol. Chem.* 266:623–629.
9. Davletov, B. A., and T. C. Sudhof. 1993. A single C2 domain from synaptotagmin I is sufficient for high affinity Ca^{2+}/phospholipid binding. *J. Biol. Chem.* 268:26386–26390.
10. Davis, A. F., J. Bai, D. Fasshauer, M. J. Wolowick, J. L. Lewis, and E. R. Chapman. 1999. Kinetics of synaptotagmin responses to Ca^{2+} and assembly with the core SNARE complex onto membranes. *Neuron.* 24:363–376.
11. Sutton, R. B., B. A. Davletov, A. M. Berghuis, T. C. Sudhof, and S. R. Sprang. 1995. Structure of the first C2 domain of synaptotagmin I: a novel Ca^{2+}/phospholipid-binding fold. *Cell.* 80:929–938.
12. Chapman, E. R., and A. F. Davis. 1998. Direct interaction of a Ca^{2+}-binding loop of synaptotagmin with lipid bilayers. *J. Biol. Chem.* 273:13995–14001.
13. Bai, J., C. A. Earles, J. L. Lewis, and E. R. Chapman. 2000. Membrane-embedded synaptotagmin penetrates *cis* or *trans* target membranes and clusters via a novel mechanism. *J. Biol. Chem.* 275:25427–25435.
14. Fernandez, I., D. Arac, J. Ubach, S. H. Gerber, O. Shin, Y. Gao, R. G. Anderson, T. C. Sudhof, and J. Rizo. 2001. Three-dimensional structure of the synaptotagmin 1 C2B-domain. Synaptotagmin 1 as a phospholipid binding machine. *Neuron.* 32:1057–1069.
15. Desai, R. C., B. Vyas, C. A. Earles, J. T. Littleton, J. A. Kowalchyck, T. F. Martin, and E. R. Chapman. 2000. The C2B domain of synaptotagmin is a Ca^{2+}-sensing module essential for exocytosis. *J. Cell Biol.* 150:1125–1136.
16. Tucker, W. C., and E. R. Chapman. 2002. Role of synaptotagmin in Ca^{2+}-triggered exocytosis. *Biochem. J.* 366:1–13.

17. Zhang, J. Z., B. A. Davletov, T. C. Sudhof, and R. G. Anderson. 1994. Synaptotagmin I is a high affinity receptor for clathrin AP-2: implications for membrane recycling. *Cell*. 78:751–760.

18. Sheng, Z. H., C. T. Yokoyama, and W. A. Catterall. 1997. Interaction of the synprint site of N-type Ca^{2+} channels with the C2B domain of synaptotagmin I. *Proc. Natl. Acad. Sci. USA*. 94:5405–5410.

19. Chapman, E. R., R. C. Desai, A. F. Davis, and C. K. Tornehl. 1998. Delineation of the oligomerization, AP-2 binding, and synprint binding region of the C2B domain of synaptotagmin. *J. Biol. Chem.* 273: 32966–32972.

20. Bai, J., W. C. Tucker, and E. R. Chapman. 2004. PIP_2 increases the speed-of-response of synaptotagmin and steers its membrane penetration activity toward the plasma membrane. *Nat. Struct. Mol. Biol.* 11:36–44.

21. Littleton, J. T., J. Bai, B. Vyas, R. Desai, A. E. Baltus, M. B. Garment, S. D. Carlson, B. Ganetzky, and E. R. Chapman. 2001. Synaptotagmin mutants reveal essential functions for the C2B domain in Ca^{2+}-triggered fusion and recycling of synaptic vesicles *in vivo*. *J. Neurosci.* 21:1421–1433.

22. Schiavo, G., Q. M. Gu, G. D. Prestwich, T. H. Sollner, and J. E. Rothman. 1996. Calcium-dependent switching of the specificity of phosphoinositide binding to synaptotagmin. *Proc. Natl. Acad. Sci. USA*. 93:13327–13332.

23. Chapman, E. R., S. An, J. M. Edwardson, and R. Jahn. 1996. A novel function for the second C2 domain of synaptotagmin. Ca^{2+}-triggered dimerization. *J. Biol. Chem.* 271:5844–5849.

24. Tucker, W. C., T. Weber, and E. R. Chapman. 2004. Reconstitution of Ca^{2+}-regulated membrane fusion by synaptotagmin and SNAREs. *Science*. 304:435–438.

25. Tucker, W. C., J. M. Edwardson, J. Bai, H. J. Kim, T. F. Martin, and E. R. Chapman. 2003. Identification of synaptotagmin effectors via acute inhibition of secretion from cracked PC12 cells. *J. Cell Biol.* 162: 199–209.

26. Bhalla, A., M. C. Chicka, W. C. Tucker, and E. R. Chapman. 2006. $Ca(^{2+})$-synaptotagmin directly regulates t-SNARE function during reconstituted membrane fusion. *Nat. Struct. Mol. Biol.*

27. Lu, X., Y. Xu, F. Zhang, and Y. K. Shin. 2006. Synaptotagmin I and $Ca(^{2+})$ promote half fusion more than full fusion in SNARE-mediated bilayer fusion. *FEBS Lett.* 580:2238–2246.

28. Earles, C. A., J. Bai, P. Wang, and E. R. Chapman. 2001. The tandem C2 domains of synaptotagmin contain redundant Ca^{2+} binding sites that cooperate to engage t-SNAREs and trigger exocytosis. *J. Cell Biol.* 154:1117–1123.

29. Zhang, X., M. J. Kim-Miller, M. Fukuda, J. A. Kowalchyk, and T. F. Martin. 2002. Ca^{2+}-dependent synaptotagmin binding to SNAP-25 is essential for Ca^{2+}-triggered exocytosis. *Neuron*. 34:599–611.

30. Bai, J., C. T. Wang, D. A. Richards, M. B. Jackson, and E. R. Chapman. 2004. Fusion pore dynamics are regulated by synaptotagmin*t-SNARE interactions. *Neuron*. 41:929–942.

31. Bhalla, A., W. C. Tucker, and E. R. Chapman. 2005. Synaptotagmin isoforms couple distinct ranges of Ca^{2+}, Ba^{2+}, and Sr^{2+} concentration to SNARE-mediated membrane fusion. *Mol. Biol. Cell*. 16:4755–4764.

32. Bai, J., P. Wang, and E. R. Chapman. 2002. C2A activates a cryptic Ca^{2+}-triggered membrane penetration activity within the C2B domain of synaptotagmin I. *Proc. Natl. Acad. Sci. USA*. 99:1665–1670.

33. Wu, Y., Y. He, J. Bai, S. R. Ji, W. C. Tucker, E. R. Chapman, and S. F. Sui. 2003. Visualization of synaptotagmin I oligomers assembled onto lipid monolayers. *Proc. Natl. Acad. Sci. USA*. 100:2082–2087.

34. Rufener, E., A. A. Frazier, C. M. Wieser, A. Hinderliter, and D. S. Cafiso. 2005. Membrane-bound orientation and position of the synaptotagmin C2B domain determined by site-directed spin labeling. *Biochemistry*. 44:18–28.

35. Fernandez-Chacon, R., A. Konigstorfer, S. H. Gerber, J. Garcia, M. F. Matos, C. F. Stevens, N. Brose, J. Rizo, C. Rosenmund, and T. C. Sudhof. 2001. Synaptotagmin I functions as a calcium regulator of release probability. *Nature*. 410:41–49.

36. Wang, P., C. T. Wang, J. Bai, M. B. Jackson, and E. R. Chapman. 2003. Mutations in the effector binding loops in the C2A and C2B domains of synaptotagmin I disrupt exocytosis in a non-additive manner. *J. Biol. Chem.* 278:47030–47037.

37. Osborne, S. L., J. Herreros, P. I. Bastiaens, and G. Schiavo. 1999. Calcium-dependent oligomerization of synaptotagmins I and II. Synaptotagmins I and II are localized on the same synaptic vesicle and heterodimerize in the presence of calcium. *J. Biol. Chem.* 274: 59–66.

38. Chapman, E. R., P. I. Hanson, S. An, and R. Jahn. 1995. Ca^{2+} regulates the interaction between synaptotagmin and syntaxin 1. *J. Biol. Chem.* 270:23667–23671.

39. Zhang, X., J. Rizo, and T. C. Sudhof. 1998. Mechanism of phospholipid binding by the C2A-domain of synaptotagmin I. *Biochemistry*. 37:12395–12403.

40. Chapman, E. R., and R. Jahn. 1994. Calcium-dependent interaction of the cytoplasmic region of synaptotagmin with membranes. Autonomous function of a single C2-homologous domain. *J. Biol. Chem.* 269:5735–5741.

41. Hudson, E. N., and G. Weber. 1973. Synthesis and characterization of two fluorescent sulfhydryl reagents. *Biochemistry*. 12:4154–4161.

42. Abrams, F. S., A. Chattopadhyay, and E. London. 1992. Determination of the location of fluorescent probes attached to fatty acids using parallax analysis of fluorescence quenching: effect of carboxyl ionization state and environment on depth. *Biochemistry*. 31:5322–5327.

43. Chung, L. A., J. D. Lear, and W. F. DeGrado. 1992. Fluorescence studies of the secondary structure and orientation of a model ion channel peptide in phospholipid vesicles. *Biochemistry*. 31:6608–6616.

44. McIntosh, T. J., and P. W. Holloway. 1987. Determination of the depth of bromine atoms in bilayers formed from bromolipid probes. *Biochemistry*. 26:1783–1788.

45. Sutton, R. B., J. A. Ernst, and A. T. Brunger. 1999. Crystal structure of the cytosolic C2A–C2B domains of synaptotagmin III. Implications for Ca^{2+}-independent SNARE complex interaction. *J. Cell Biol.* 147:589–598.

46. Brose, N., A. G. Petrenko, T. C. Sudhof, and R. Jahn. 1992. Synaptotagmin: a calcium sensor on the synaptic vesicle surface. *Science*. 256:1021–1025.

47. Zhou, H. X. 2003. Quantitative account of the enhanced affinity of two linked scFvs specific for different epitopes on the same antigen. *J. Mol. Biol.* 329:1–8.

48. Frazier, A. A., C. R. Roller, J. J. Havelka, A. Hinderliter, and D. S. Cafiso. 2003. Membrane-bound orientation and position of the synaptotagmin I C2A domain by site-directed spin labeling. *Biochemistry*. 42:96–105.

49. Damer, C. K., and C. E. Creutz. 1994. Synergistic membrane interactions of the two C2 domains of synaptotagmin. *J. Biol. Chem.* 269: 31115–31123.

50. Damer, C. K., and C. E. Creutz. 1996. Calcium-dependent self-association of synaptotagmin I. *J. Neurochem.* 67:1661–1668.

51. Mackler, J. M., J. A. Drummond, C. A. Loewen, I. M. Robinson, and N. E. Reist. 2002. The C2B Ca^{2+}-binding motif of synaptotagmin is required for synaptic transmission *in vivo*. *Nature*. 418:340–344.

52. Stevens, C. F., and J. M. Sullivan. 2003. The synaptotagmin C2A domain is part of the calcium sensor controlling fast synaptic transmission. *Neuron*. 39:299–308.

53. Nishiki, T., and G. J. Augustine. 2004. Dual roles of the C2B domain of synaptotagmin I in synchronizing Ca^{2+}-dependent neurotransmitter release. *J. Neurosci.* 24:8542–8550.

54. Rhee, J. S., L. Y. Li, O. H. Shin, J. C. Rah, J. Rizo, T. C. Sudhof, and C. Rosenmund. 2005. Augmenting neurotransmitter release by enhancing the apparent Ca^{2+} affinity of synaptotagmin 1. *Proc. Natl. Acad. Sci. USA*. 102:18664–18669.